# Bubble number density of pumice and ash of the Aira pyroclastic eruption: estimate from bubble wall thickness

**Yoshie OKI, Tatsuyuki UENO, Hiroaki SATO, Keiko SUZUKI-KAMATA**
Department of Earth and Planetary Sciences, Faculty of Science and Graduate School of Science and Technology, Kobe University, Rokko-dai 1-1, Nada-ku, Kobe, 657-8501, JAPAN
(correspondence: hsato@kobe-u.ac.jp)

## 1. Introduction

Pumice and ash constitute pyroclastic materials, which may record the vesiculation/fragmentation processes of magmas during explosive eruptions. By the numerical calculation of vesiculation processes at constant ascent rate of magmas, Toramaru (1995) pointed out that the bubble number density is proportional to the 3/2 power of the decompression rate for homogeneous nucleation of bubbles. This relationship is recently verified by the experimental studies of Mouritada-Bonnefoi & Laporte (2004). Therefore, we expect to extract the decompression rate from bubble number density of pyroclasts. Vesicle textures of natural pyroclastic material have been described by many workers. Toramaru (1990) described two methods of measurement of bubble number density and other parameters of vesicle textures. Klug et al. (2002) measured the bubble size distribution and bubble number density on the ejecta of Mt. Mazama caldera-forming eruptions. These researchers, however, tried to analyze vesicle textures only for pumice fragments. Pumice fragments illustrates marked vesicle textures, although they generally constitutes less than half of the ejecta of a pyroclastic eruption. Ash (less than 2 mm in diameter in definition) constitutes half to two third of ejecta of pyroclastic eruptions. Cursory examination of vesicle textures of pumice and ash of large scale eruption products often shows that bubble wall thicknesses of pumice and ash are much different (e.g. Machida and Arai, 1992). We describe here the vesicle textures in terms of grain size of pyroclasts of a caldera-forming pyroclastic eruption of Aira caldera 25 ka. We focused on the bubble-wall thickness for the comparison of vesicle textures of pumice and ash, which reflect the bubble size and number density of the pyroclasts.

## 2. Method and Calibration

Assuming the bubble cell model of Proussevitch and Sahagian (1996), the bubble wall thickness (d) is proportional to vesicle size for constant porosity (p) and also is related to the number density of vesicles (Nv), as $Nv = 6(1-p^{1/3})^3/[\pi(1-p)d^3]$. This relationship is shown in Figure 1, where the relationship of Nv to bubble wall thickness for porosity of 0.65, 0.75 and 0.85 are illustrated. For the measurement of bubble wall thickness, we arbitrarily drew straight lines in a back-scattered electron image of a section of pyroclasts, and measured the apparent thickness of bubble wall where the lines meet the center line of a bubble wall. More than 300 bubble wall thicknesses are counted for each sample, and the number of walls (N) in each class with $2^n$ microns is obtained. We assumed random 3D orientation of bubble walls, and corrected for the effect of measuring apparent thickness (oblique cutting effect) by reducing the number of walls for larger class from the number of walls for smaller class. The number density of bubble is obtained by summation of all the N for each class from the above equation assuming the

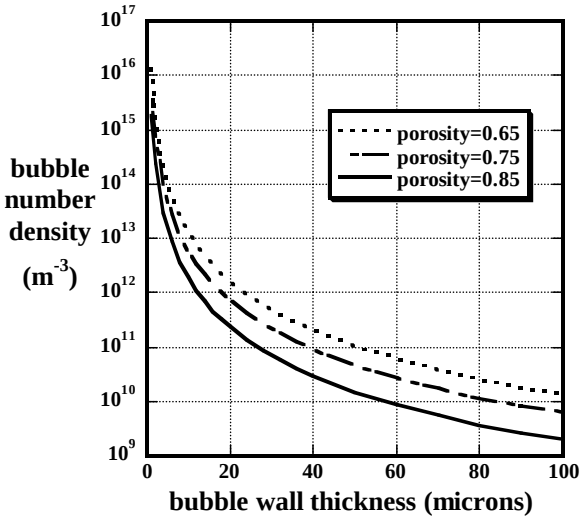


Figure 1 Bubble number density (Nv) versus bubble wall thickness assuming bubble cell model.

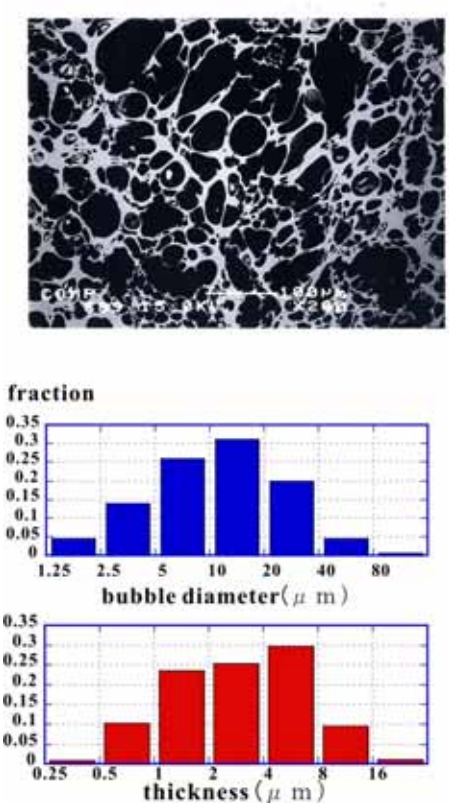


Figure 2 An example of measurement of bubble and calibration against bubble area measurements

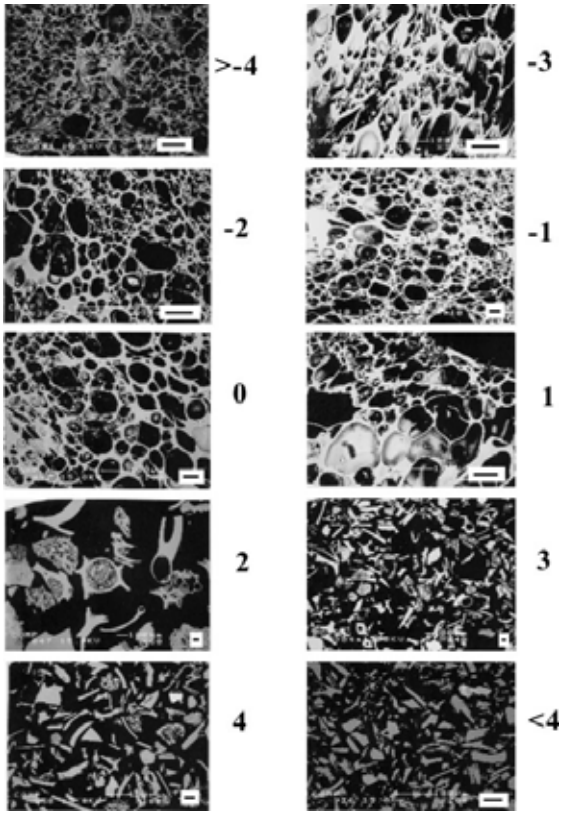


Figure 3 Back scattered electron images of pyroclasts of Ito pyroclastic flow deposit. Numbers attached to the pictures denote the phi scale range; i.e., -2 means the grain size range of -3 to -2 phi, corresponding to 8 to 4 mm across. Scales represent 50 microns.

vesicularity of 0.8 for ash fragments. This method is calibrated against the measurement by other methods of Toramaru (1990), and showed good correspondence (Fig. 2).

## 3. Samples and Results

We selected three samples of the Aira pyroclastic eruption products; i.e., Osumi pyroclastic fall deposit; Ito pyroclastic flow deposit, and AT co-ignimbrite deposit. These samples were sieved to obtained grain size distributions. We then made polished thin sections for different grain size from -4 phi to <4 phi, for which back scattered electron images were obtained for measurement of bubble wall thickness. Even in a class of grain size for a deposit, pumice may show variation of vesicle texture. So we measured seven pumice clast of the same grain size class of Ito pyroclastic flow deposit. They showed some variation in bubble wall thickness, and Nv calculated for the pumice clast varied from $1.3*10^{14}$ to $5.8*10^{14}$ $m^{-3}$ with a standard error of $1.3*10^{14}$ $m^{-3}$. Figure 3 shows the distribution of bubble wall thickness for the three samples. The average bubble wall thickness varies by more than 1 order of magnitude according to the grain size of the pyroclasts, ranging from less than 3 microns thick for pumices of Osumi pumice fall deposit (-2-0 phi) up to 30 microns thick for bubble wall ash of AT co-ignimbrite ash (1-4 phi), corresponding to bubble number densities of $5\text{-}12*10^{14}$ and $3\text{-}5*10^{12}$ $m^{-3}$, respectively (we assumed p=0.80; Figure 4). Although we have no data on the vesicularity of pyroclasts in the formation of the bubble-wall glass ash, its low width/length ratio suggests high vesicularity similar to the pumice components. Figure 3 also indicates that average bubble wall thickness generally increases in the stratigraphic succession; i.e., from Osumi pumice fall deposite through Ito pyroclastic flow deposit to AT co-ignimbrite ash deposit. Bubble number density calculated from the bubble wall thickness, presented in Figure 4, also show that Nv is generally higher for the early ejecta of Osumi pumice fall deposite, whereas the

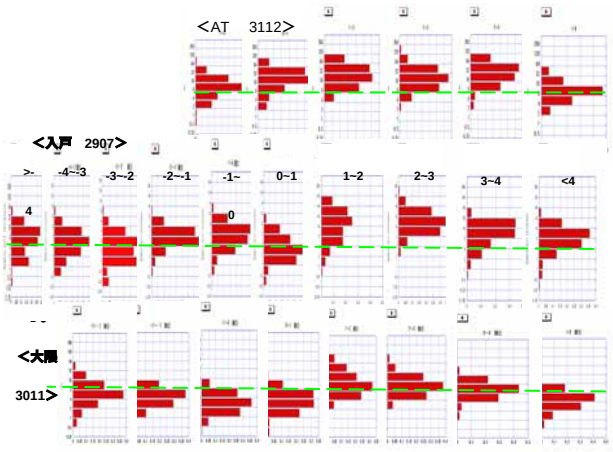


Figure 4 Measurement of bubble wall thickness for the three samples according to the grain size. The upper diagrams show the distributions of bubble wall thickness for coarse-grained (left) to fine-grained pyroclasts of AT co-ignimbrite deposit, the middle diagrams show those of Ito pyroclastic flow deposit, and the lower diagrams show those of Osumi pumice-fall deposit.

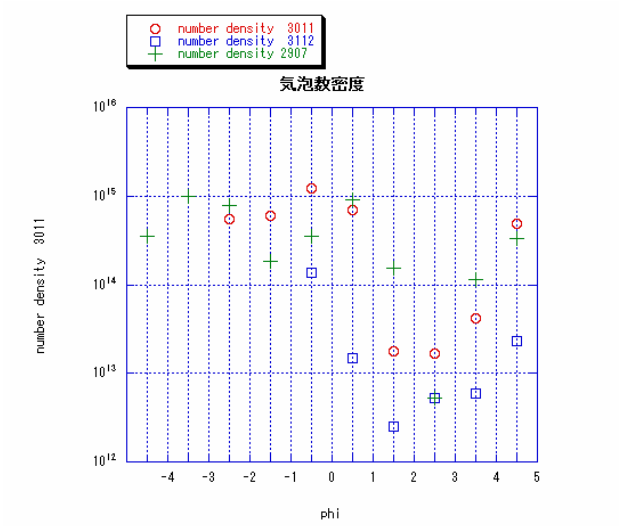


Figure 5 Bubble number density(Nv) of pyroclasts according to the grain size of pyroclasts. Note markedly lower Nv for phi scales of 1-3, corresponding to the bubble wall glass, compared with pumice fragments of phi greater than 0. Open circle: Osumi pumice fall deposit, open square: AT co-ignimbrite deposit, cross: Ito pyroclastic flow deposit.

last co-ignimbrite ash has the lowest Nv. Figure 5 also illustrates the higher Nv for pumice (<0 phi) compared with bubble wall ash (1-4 phi) by 1 to 2 orders of magnitude. Difference in bubble number density between pumice and bubble-wall glass ash indicates that the mode of vesiculation and fragmentation during the ascent of magmas is different for the pumice-forming magma and the ash-forming magma.

## 4. Discussion

The low number density of vesicles of the bubble-wall glass ash suggests that the decompression rate of the corresponding magma would be small (Toramaru, 1995; Mourtada-Bonnefoi and Laporte, 2004), which is somewhat odd to the presumed rapid magma ascent during caldera-forming eruptions. Three possible causes of the low number density of vesicles for the bubble-wall glass ash are suggested; i.e., (1) large oversaturation of water due to rapid decompression suppressed the bubble nucleation, (2) vesiculation occurred under small water-oversaturation due to slow decompression in the conduit during the caldera-forming pyroclastic flow eruption, (3) vesicle nucleation started in the magma chamber, where low oversaturation caused low number density of vesicles, and subsequent expansion of vesicles during rapid ascent in the conduit. We discuss these models briefly in the followings.

In the case of crystallization, large undercooling and oversaturation may suppress the crystal nucleation. However, in the case of vesicualtion, it is unlikely that large oversaturation suppress the vesicle nucleation because large oversaturation may decrease the critical radius of vesicles for vesicle nucleation, and there may be no reason for changing the cluster size distribution of water in the melt due to large depressurization. Therefore the model (1) may be unlikely. The model (2) is apparently at odd in terms of large eruption rate of caldera-forming eruptions. Because the numerical study of Toramaru (1995) and experimental study of Mouritada-Bonnefoi and Laporte showed that bubble number density is proportional to the 3/2 power of decompression rate of magmas, the low bubble number density of ash in the large pyroclastic eruption like Aira suggest low decompression rate. Carey and Sigurdsson (1989) estimated that eruption rate of Osumi pumice fall was $4.2*10^8$ kg/s, which is one of the largest value amongst ca. 50 large explosive eruptions in the list. However, because the caldera-forming eruption may have large cross sectional area of the vent, large eruption rate does

not necessarily mean that the decompression rate was large. The low Nv observed for the bubble-wall ash fragments in the Aira pyroclastic eruption products indicates that the decompression rate of the magma was actually small compared with the pumice-forming eruptions such as Towada volcano (Toramaru, 1990).

## References


Aramaki, S. (1984) Formation of the Aira Caldera, southern Kyushu, 22,000 years ago. J. Geophys. Res., 89, 8485-8501.

Carey, S., Sigurdsson, H. (1989) The intensity of plinian eruptions. Bull. Volcanol., 51, 28-40.

Klug, C., Cashman, K.V., Bacon, C.R. (2002) Structure and physical properties of pumice from the climactic eruption of Mount Maama (Crater Lake), Oregon. Bull. Volcanol., 64, 486-501.

Machida, H. and Arai, F. (1992) Atlas of Tephras in and around Japan. Univ. Tokyo Press, 276p.

Mourtada-Bonnefoi, CC., Laporte, D. (2004) Kinetics of bubble nucleation in a rhyolitic melt: an experimental study of the effect of ascent rate. Earth Plan. Sci. Lett., 218, 521-537.

Proussevitch, AA, Sahagian, DL (1996) Dynamics of coupled diffusion and decompressive bubble growth in magmatic systems. Journal of Geophysical Research, 101, 17447-17455.

Sato, H., Ueno, T., Suzuki-Kamata, K., Oki, Y. (2005) Bubble wall thickness as a measure of bubble number density of pyroclasts: implications for bubble-wall glass ash in a caldera-forming pyroclastic flow eruption of Shikotsu volcano, Japan. Abstract Volume of International workshop on volcanic explosion in Kobe, Japan, p69.

Toramaru, A. (1990) Measurement of bubble-size distributions in vesiculated rocks with implications for quantitative estimation of eruption processes. J. Volcanol. Geotherm. Res., 43, 71-90.

Toramaru, A. (1995) Numerical study of nucleation and growth of bubbles in viscous magmas. J. Geophys. Res., 100, 1913-1931.

Ueno, T. (2004) Eruption mechanism of a large-scale pyroclastic flow: A case study of Aira pyroclastic eruption. PhD Thesis, Kobe University, 165p.